ACS OMEGA

Open Access

http://pubs.acs.org/journal/acsodf

Article

Design, Synthesis, and Characterization of HBP-Vectorized Methotrexate Prodrug Molecule 1102−39: Evaluation of In Vitro Cytotoxicity Activity in Cell Culture Models, Preliminary In Vivo Safety and Efficacy Results in Rodents

Maxim Egorov,* Jean-Yves Goujon, Marie Sicard, Christelle Moal, Samuel Pairel, and Ronan Le Bot

Cite This: *ACS Omega* 2024, 9, 42433−42447

Read Online

ACCESS | Metrics & More | Article Recommendations | Supporting Information

ABSTRACT: A novel bone-targeted prodrug, 1102−39, is discussed with the aim of enhancing the therapeutic effects of methotrexate (MTX) within bone tissues while minimizing systemic toxicity. Within the 1102−39 molecule, the central linker part forms a cleavable ester group, with MTX being also linked by a stable imine bond to the specially designed hydroxybisphosphonic (HBP) vector. Synthesized through a convergent approach starting from MTX, this prodrug advantageously modulates MTX's activity by selective esterification of its α-carboxyl group. In vitro tests revealed a 10-fold reduction in cytotoxicity compared to standard MTX, in alignment with prodrug behavior and correlated with gradual MTX release. In vivo in rodents, 1102−39 displayed preliminary encouraging antitumor effects on orthotopic osteosarcoma. Furthermore, various aspects of designing molecules for selective therapy in bone tissue based on bisphosphonate molecules as vectors for delivering active compounds to the bone are discussed. The 1102−39 molecule exhibits strong affinity for hydroxyapatite and a progressive release of MTX in aqueous environments, enhancing the safety and efficacy of bone-specific treatments and enabling sustained activity within bone and bone joints in the therapy of tumor and inflammation.

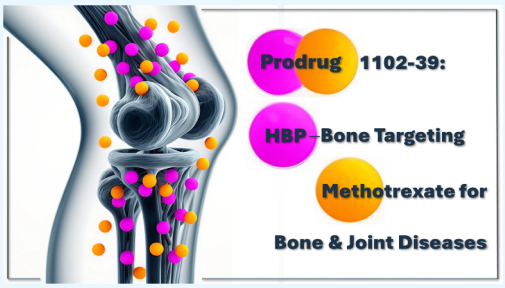

INTRODUCTION

Methotrexate (MTX) is an antifolate drug with antiproliferative and anti-inflammatory effects. MTX proved to be the most highly effective, fast-acting disease-modifying antirheumatic drug (DMARD), being widely used for the treatment of rheumatoid arthritis (RA).

Methotrexate (MTX) [registered as Imeth, Novatrex, and generics] is a crucial therapy agent, acknowledged as a fundamental element in both cancer treatment[1,2] and rheumatology.[3,4] MTX's potency against cancer originates from its strong inhibition of dihydrofolate reductase (DHFR), leading to the depletion of essential tetrahydrofolates required for purine synthesis and thymidylate synthase crucial for RNA and DNA production.[2] To overcome the development of cancer resistance to MTX, it is often administered in high, sometimes life-threatening, doses — particularly risky for adults.[5] Vigilant monitoring for signs of toxicity and timely application of the rescue agent are essential.[1] At the same time, low-dose MTX could exhibit more anti-inflammatory than antiproliferative effects on cells responsible for joint inflammation in rheumatoid arthritis. This modulation arises from inhibiting folate-dependent enzymes, potentially resulting in immunosuppression.[2] MTX can also inhibit leukocyte multiplication and function,[6] reduce cytokine production, trigger the release of anti-inflammatory adenosine, and hinder amino acid interconversions.[7] In the treatment of rheumatoid arthritis (RA), MTX stands as the primary first-line disease-modifying antirheumatic drug (DMARD). However, at common effective doses, MTX induces significant systemic side effects in around 80% of patients, leading to a pause in therapy in about 35% of cases.[8] More recently, a double-blind, randomized, and controlled versus placebo clinical trial (registered in the Australian New Zealand Registry (ACTRN12617000877381)), conducted on 202 patients (aged 40 to 75) with osteoarthritis of the hand and synovitis detected by MRI, showed that MTX (20 mg once a week for 6 months) had a moderate but potentially clinically significant effect on pain reduction. However, despite MTX being indicated in the treatment of psoriasis, psoriatic rheumatism, and rheumatoid arthritis, overdoses (several times a week) and drug interactions (with non-steroidal anti-inflammatory drugs (NSAIDs) and proton pump inhibitors (PPIs)) are frequent,

Received: June 29, 2024
Revised: September 5, 2024
Accepted: September 10, 2024
Published: October 2, 2024

warns the health authorities, which reminds that MTX should be administered only once a week.[9]

In addition, a meta-analysis based on relevant articles from randomized controlled trials published until March 2022 in PubMed, Embase, and Cochrane Library databases was carried out in compliance with the PRISMA 2020 recommendations. Overall, the available data on the effects of disease-modifying antirheumatic drugs (DMARD) on the intensity of OA symptoms are disappointing but points out that only methotrexate could have an analgesic effect, especially in gonarthrosis, justifying further studies.[10]

As a result, despite the effectiveness of MTX, its clinical use is hindered by dose-related toxicity, linked to its short half-life in the bloodstream and rapid and uniform tissue distribution.[11]

Future pharmacotherapy could be enhanced by directing toxic agents to specific pathological sites, thus improving the therapeutic index and preventing significant side effects.[12] Approximately 20% of drugs approved post-2000 are prodrugs, primarily engineered to reduce and overcome unfavorable aspects such as absorption, distribution, metabolism, excretion, and toxicity (ADMET).[4]

Different approaches to enhance the MTX therapeutic profile through various nonbisphosphonic (BP) delivery systems such as albumin,[13,14] liposomes,[8,15] microspheres, chitosan nanoparticles,[16] dendrimers,[17] lipid nanoparticles,[18] and nanostructured lipid carriers[19] provide prolonged plasma profile, and enhanced and specific activity in vitro and in vivo in animal models.[2] MTX conjugates with poly(L-lysine), dextran,[20] hyaluronic acid,[3] and peptides,[12,21,22] alongside nanoparticles,[23] phospholipids,[24] and nanotubes[25] have been synthesized. MTX-loaded materials, such as acrylate cement for local bone metastasis therapy, have also been reported.[26,27] Tumor-targeting methotrexate-antibody conjugates demonstrated partial success and faced limitations of low charge with MTX.[1] Periodically, the solubility of the final methotrexate conjugates and MTX release are unsuitable.[28] Structurally, polymer-supported MTX lacks the strict organization and composition that individual molecules possess; however, they do highlight the utility of MTX vectorization.

All the mentioned MTX vectorizations do not target bone tissue, despite its frequent involvement in tumoral and articular inflammatory pathologies. MTX distribution within bones and bone joints is hindered by low blood flow and the blood−bone marrow barrier, constituted of lining cells.[29] Selective MTX targeting toward pathological bone sites through vectorization could slow its metabolism, enhance therapeutic effectiveness, reduce administered doses (quantity and frequency), minimize systemic exposure, and increase local effective concentrations.[30,31] This is particularly important, as diseases like osteosarcoma exhibit poor responses to conventional methotrexate doses but are responsive to high-dose methotrexate.[32] Bone targeting offers a means to improve the therapeutic index and allows less frequent administration.[33,34]

The strong affinity of bisphosphonates to bone tissue[35] and their application in developing bone-targeting medications have been confirmed by numerous studies in the fields of oncology, infectious diseases, and inflammatory pathologies. Indeed, after intravenous administration of a bisphosphonate, approximately 50−75% of the injected dose binds to exposed bone mineral, with half-lives in the blood circulation in the range of 0.5−6 h in humans depending on the bisphosphonate and administered dose. Table 1 provides an overview of reported bisphosphonic (BP) and hydroxybisphosphonic (HBP) prodrugs containing potentially cleavable API-releasing groups.

Bisphosphonates are nonhydrolyzable pyrophosphate analogs with a high affinity for hydroxyapatite (HA) in bone tissue. They can inhibit osteoclast activity and bone resorption, with the efficacy depending on their structure.[30,72] An important feature of bisphosphonates is that the uptake in pathological bone tissue can be 10−20 fold higher than in healthy bone tissue.[47] This is particularly relevant in cases of cancerous and inflammatory processes, which lead to accelerated bone remodeling, often establishing a positive feedback loop favorable for the pathology development.[73] Additionally, these processes involve extracellular matrix formation[73] and osteolysis,[74] resulting in the exposure of a significantly active HA bone surface that effectively binds bisphosphonates.[30]

Bisphosphonate (BP) conjugates containing anti-inflammatory active pharmaceutical ingredients (APIs) have a limited presence in the literature. Only a few examples of such conjugates have been reported, which include methotrexate (MTX) derivatives,[75−77] cortisone,[45] ibuprofen,[61,68] diclofenac,[46,47] and meloxicam.[67] Notably, the last two cases highlight the release of APIs and the in vivo anti-inflammatory effectiveness (iv administration) without the typical gastrointestinal side effects associated with nonsteroidal anti-inflammatory drugs. In the diclofenac case, this achievement is accompanied by a substantial 4-fold reduction in the molar therapeutic dose, while in the meloxicam case, a single injection achieves sustained efficacy for one month, eliminating the necessity of daily dosing.[67]

The reported anticancer effects of BP MTX derivatives[75] and the HBP ALN-PEG-MTX dendrimer[29] encourage further investigation into bone-targeting BP MTX derivatives.

Within the scope of this work, we present the synthesis of a methotrexate hydroxybisphosphonate (HBP) prodrug, designated as a 1102−39 molecule (Figure 1). This prodrug is designed for localized MTX release within bone tissue, intended to treat osteo-articular pathologies, including bone cancer and bone joint inflammation.

RESULTS AND DISCUSSION

Despite the long-known bone affinity of bisphosphonates, the number of bisphosphonate molecules capable of releasing active substances in the bone/bone joint remains relatively limited, as shown in Table 1. This shortage can be largely attributed to the challenges in producing complex cleavable polar and chelating bisphosphonate molecules, as well as their difficult manipulation and purification. Some of these molecules were previously reviewed.[31,37,74] In recent publications, we emphasized the effectiveness of the HBP-vectorized doxorubicin molecule 12B80[64] in rodent models[65] and canine models.[78] Additionally, we reported on the HBP-vectorized NSAID meloxicam cleavable 18A184 molecule, which exhibited sustained antiarthritic activity in rats without side effects[67] and demonstrated a safe toxicity profile in dogs (unpublished data).

Molecules with a noncleavable API-vector bond are more readily accessible synthetically, and therefore they were historically among the first explored. Although these stable molecules cannot serve as prodrugs and typically lack activity, they may rarely exhibit nonspecific effects, as in the case of vectorized alkylating agents,[79,80] or even interactions with a target.[81] Noncleavable molecules can hold interest, like in

https://doi.org/10.1021/acsomega.4c06029
ACS Omega 2024, 9, 42433−42447

Table 1. List of Bisphosphonic and Hydroxybisphosphonic Prodrugs Containing Potentially Cleavable API-Releasing Groups

API-releasing group	BP	HBP
imine	Doxorubicin[37]	Alkylating agents[61]Doxorubicin[61,63−65]Estrone[61]
carbamate	Doxorubicin[37]Gemcitabine[38−40]Vancomycin[44]Chloroquine[49]Vitamins D2 and D3[50]Estradiol[54] Fluoroquinolones[56]Ciprofloxacin[57,58]	Alkylating agents[61]Podophyllotoxin[61]Rapamycin[66]PGE2 analogs[89]Benzocain[61]
ester	Camptothecin[36]Vancomycin[44]Cortisone[45]Diclofenac[46,47]PGE2[48]Estradiol[33,34,51−53]Fluoroquinolones[55]Benzoxazinorifamycin[59]	Methotrexate[61]SN38[61]Meloxicam[67]Ibuprofen[61,68]PGE2 analogs[69−71]
thioester	PGE2[48]Fluoroquinolones[55]	Nucleotide analogs[41−43]Alkylating agents[60]Cytarabine[62]Meloxicam[67]
phosphate	Nucleotide analogs[41−43]	Nucleotide analogs[41−43]Cytarabine[62]
pyrophosphonate sulfonate	Nucleotide analogs[41−43]	Meloxicam[67]

instances where HBP vectorized cyclodextrin is charged with an API and can release it.[82] As a result, nearly the only-possible strategy is the use of cleavable molecules, which implies the release of active compounds from prodrug vectors to induce a biological response through specific target interactions. Often, it proves to be more effective than the standalone API as it is the case of BP-vectorized diclofenac,[46,47] gemcitabine,[38−40] fluoroquinolones,[55,57,58] or HBP-vectorized nucleotide analogs,[42,62] as well as HBP-vectorized doxorubicin[65,78] and NSAID meloxicam.[67]

The rate of API release is crucial to ensure activity[59] and should be checked even in the case of such theoretically cleavable API-binding groups as ester, carbamate, imine, and so on, as it may be insufficient depending on the characteristics of both the active molecule and the linker-vector part.[51,54−56,69]

Cleavable API-BP derivatives are more explored in vivo, while API-HBP cleavable molecules have limited representation (Table 1), including our contributions based on eight publications.[60,61,64,65,67,78,83,84] Among the reported API-HBP cleavable molecules, only few have undergone in vivo studies, especially one clinical Phase I trial[62] and two involving rodents and dogs.[65,67,78] This difference between BP and HBP arises from the greater synthetic accessibility of BPs compared to that of HBPs. Over the years, we have been actively working on developing new synthetic methods (as previously indicated) to create multifunctional HBP molecules, thus, expanding their availability for research and practical applications.

Synthesis and Structure. *Structure and Concept.* The 1102−39 molecule consists of three key parts: the central linker forms a cleavable ester releasing group with MTX and is connected from the other side to the vector through a stable imine bond (Figure 2).

Only two groups of researchers have presented a few bisphosphonic MTX-derivative structures.[75−77] In the latter case, only a 5 mg yield of the final product is documented, with no exploration of its physicochemical or biological properties. All mentioned compounds are amide-linked bisphosphonates at the γ-carboxyl group of MTX. Among them, the most promising compound primarily targeted the bone tissue[85] and demonstrated greater in vivo anticancer activity compared to MTX alone. However, it also exhibited increased systemic toxicity.[75,76] This strategy of BP vectorization was supposed to result in several-fold higher levels of conjugated methotrexate at the bone site.[85] This supports the potential of such an approach. Based on several aspects as described below, 1102−39 is a newly modified and improved MTX molecule that targets bones (Figure 1).

First, we used a hydroxybisphosphonate vector instead of the bisphosphonate derivative (Figure 2). Hydroxybisphosphonates are recognized for their stronger bone affinity compared to bisphosphonates, attributed to the formation of a more potent tridentate complex, distinct from the bidentate complex observed with BP.[30,86,87] The introduction of a nitrogen atom in the vector's lateral chain enhances HA affinity through hydrogen bonding with surface hydroxyl groups, consequently rendering its zeta-potential more positive and attractive for negatively charged HBP binding.[30] Additionally, the naturally polar hydroxybisphosphonate group enhances the aqueous solubility.

Second, we obtained an α-carboxyl substituted derivative of methotrexate (Figure 2), which appears more suitable for the prodrug role due to its inactivity until cleavage. α-carboxyl substituted MTX derivatives are known to lose MTX activity,[15]

https://doi.org/10.1021/acsomega.4c06029
ACS Omega 2024, 9, 42433−42447

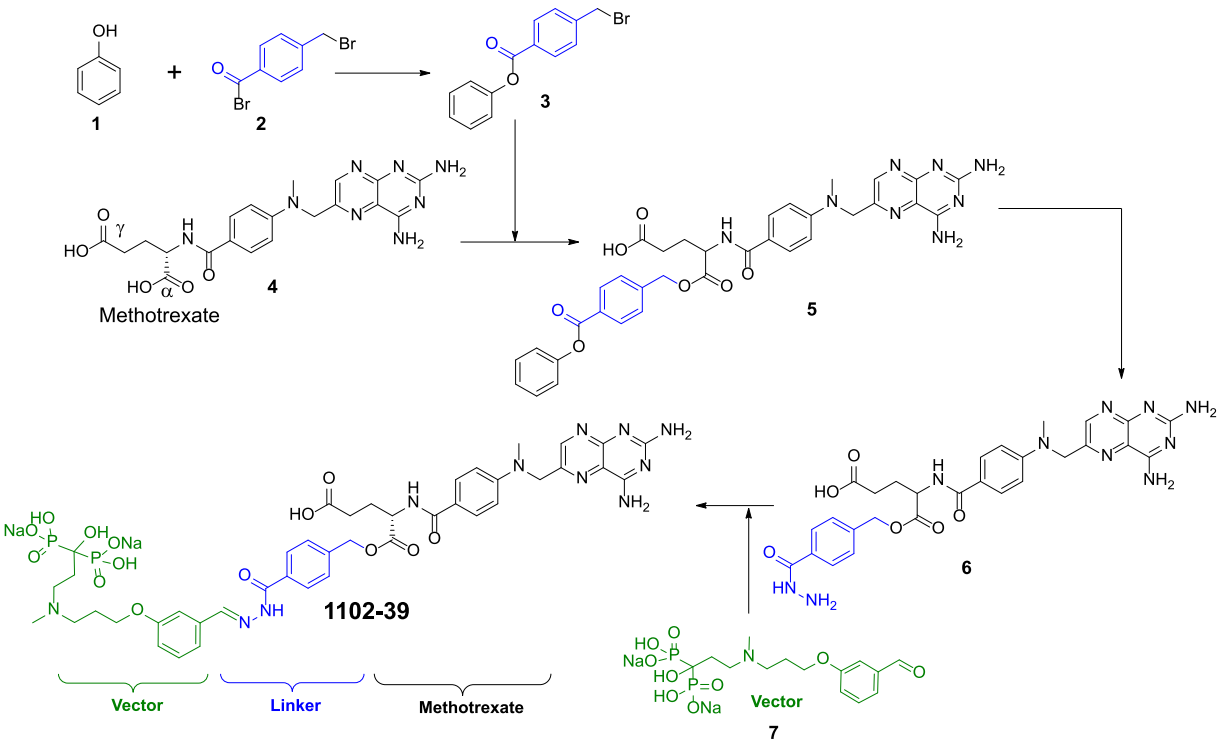

Figure 1. Synthesis scheme of the 1102−39 molecule.

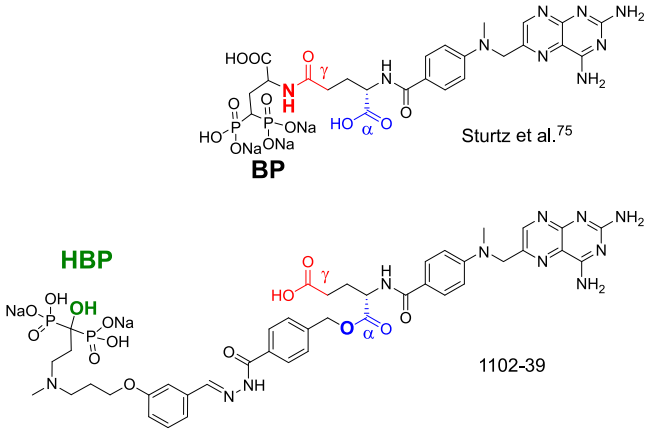

Figure 2. Improved concept of the 1102−39 molecule structure.

the α-carboxyl acting as the essential structural determinant for MTX, aiding its transport into cells[88] and its binding with DHFR.[89] In contrast, γ-carboxyl substituted derivatives maintain better MTX activity,[90,91] probably due to the γ-carboxyl of folate compounds being positioned outside the active site cavity of the target DHFR enzyme.[1] This fact could explain the antitumor activity of the mentioned γ-carboxyl substituted amide BP-MTX derivative,[75] where no evidence indicates MTX liberation by the amide group, known to be excessively stable for producing free active compounds,[48,58,92] This observation aligns with its in vitro activity, similar to MTX,[75] while in a prodrug context, it typically shows lower activity compared to native API, as demonstrated in the case of the HBP-doxorubicin,[64,65,67] and the NSAID HBP-meloxicam[67] prodrugs.

Third, we developed a method to synthesize HBP ester derivatives of methotrexate, allowing release.

Therefore, an α-carboxyl-substituted MTX ester-linked prodrug could exhibit reduced systemic activity compared to the γ-substituted one, owing limited cell uptake and local cytotoxicity through hydrolysis-mediated MTX liberation.[93] This strategy was validated through in vitro tests of the 1102−39 molecule, demonstrating a 10-fold reduction in activity compared to that of MTX, indicating significantly lower prodrug cytotoxicity and gradual MTX release.

The mentioned γ-substituted amide BP-MTX compound[75] was obtained via total synthesis of the methotrexate segment, ensuring unambiguous MTX substitution. Our efficient synthesis is based on the use of methotrexate itself as the starting material. Described here, the 1102−39 molecule is the first example of ester-bonded bisphosphonate MTX derivatives.

Convergent Synthesis Strategy. The bifunctional HBP molecules can be constructed using both linear[60,68] and convergent[61,64,65,67,68] strategies. The latter approach was preferred due to its greater convenience and suitability for complex multifunctional APIs. We employed the strategy of forming a stable imine bond with a specially developed hydroxybisphosphonate vector in the final step. In general, the imine strategy provides versatility, serving as both a releasing group, as previously described,[64,65] and a stable bond that facilitates the construction of complex molecules, as used in this work. We have previously demonstrated the effectiveness of this strategy in vectorizing various therapeutic molecules.[61,64,67]

This approach enables the direct use of bisphosphonate vector without requiring protective groups. Employing the common Cu-based click chemistry with unprotected bisphosphonates is complicated due to copper chelation with bisphosphonates.[68,94] Although protective groups are convenient for bisphosphonates,[48] they are less suitable for hydroxybisphosphonates, which tend to form phosphonate-

https://doi.org/10.1021/acsomega.4c06029
ACS Omega 2024, 9, 42433−42447

phosphate byproducts involving the free HBP C−OH group, especially in the presence of a base, high temperature, and sometimes column purification.[68,95−98] While the protection of the HBP C−OH group is known, it complicates seriously the synthesis.[97] Therefore, in summary, employing ester protection for the HBP group poses notable challenges.[97] Additionally, the deprotection methods for the BP group (even mild ones like TMSI[54,87] and particularly TMSBr[99,100] or catalytic hydrogenation) should be compatible with the final compound's stability, which is not always possible.[53,69]

Consequently, performing the final imine formation involving unprotected hydroxybisphosphonates is a good alternative. This can be achieved for our MTX-HBP 1102−39 molecule in both aqueous media[61] and anhydrous solvents, as demonstrated in this study. We specifically designed HBP vectors,[61,64,67] to efficiently accommodate the imine synthesis approach. Classic hydroxybisphosphonates like zolendronate, pamidronate, or alendronate are unsuitable for this strategy and might also initiate unwanted excessive antiosteoclastic activity if used in a one-to-one ratio with the vectorized API. We previously demonstrated the synthetic efficacy of our vectors with doxorubicin,[64] meloxicam,[67] and other APIs[61] HBP derivatives. The HBP vector used in this study displayed favorable in vivo biological profiles when used in the HBP-vectorized Doxorubicin 12B80 prodrug molecule,[65] having moderate antiosteolytic activity and a gentle enhancement of the primary therapeutic effect. This finding could facilitate the treatment of bone disorders influenced by cancer and inflammation.[49] As a result, we can fine-tune the bone affinity/antiosteoclastic activity ratio of the prodrug molecule.

HBP Vector Synthesis. Traditional techniques involving heating an appropriate carboxylic acid with phosphorus acid and phosphorus trichloride at temperatures reaching around 100 °C, followed by hydrolysis, have proven to be impractical for vector synthesis due to their harsh conditions, complex procedures, and restricted reproducibility.[72,87] Consequently, we initially employed the efficient and mild one-pot catecholborane method that we had previously discovered.[83,84] This method's effectiveness is demonstrated in various works.[60,61,64,67,68,101] We used the nucleophilic tris-(trimethylsilyl)phosphite, as suggested by Lecouvey et al., for HBP synthesis.[102] However, the conventional acylchloride activation described in this work[102] was blocked due to the presence of the basic nitrogen atom within our vector. When synthesizing analogous nitrogen-containing HBP derivatives, the same research group previously had to use the amine protection before the synthesis,[103] which is not feasible for tertiary amines, like in our vector. In contrast, our catecholborane method allows this transformation directly within a one-pot synthesis at room temperature, eliminating the need for protective groups for all amine types (and even −OH groups), as the amine nitrogen atom forms a robust complex with catecholborane, which also serves as the carboxyl group activator.[83,84] Subsequently, we discovered and used a low-temperature HBP synthesis method involving mixed anhydride with pivaloyl acid as we described earlier.[64] This strategy resulted in increased yields and scalability of the Vector,[65] though with limited generality for HBP synthesis compared to catecholborane method.

MTX Derivatization Selectivity. The MTX molecule, with multiple reaction sites, often yields several substituted MTX isomers during synthesis, posing challenges in their separation on a preparative scale.[104] This often necessitates to carry out the full synthesis of the substituted MTX moiety from unambiguously protected glutamic acid.[21,25,75,76,88,91,93,105,106]

γ-Carboxyl MTX substituted derivatives are the most explored due to their synthesis being facilitated by using bulky carboxyl group activators like TBTU, which slow down the reaction on the hindered α-carboxyl group of MTX.[28,89] We developed the synthesis of the α-substituted derivative based on the higher acidity of the α-carboxyl group (pK_a 3.36 vs 4.70 for γ-carboxyl) in methotrexate,[107] enhancing the selectivity of N-acylglutamic moiety substitution in the presence of base.[108,109] To achieve this, we coupled MTX sodium salt with benzylbromide derivative **2**, creating the ester MTX-releasing group. This chemical reaction avoids the use of reactants like DCC resulting in MTX racemization, as observed in MTX carboxyl activation case.[20,93,105] Despite improved selectivity, a mixture of mono-, di-, and trisubstituted products still forms. These isomers prove challenging to purify using traditional eluents like DCM-MeOH on silica gel columns, as noted in our earlier work.[61] In this study, we found effective separation conditions utilizing a gradient elution from DCM/Et_2O to a triple DCM/Et_2O/MeOH mixture, yielding pure final product **5** at 37% yield. This step was successfully scaled to 1 g. Further, we optimized reaction conditions for the selective hydrazinolysis of the phenyl ester in the presence of the alkyl ester MTX releasing group, leading to the precipitation of hydrazide **6** in 88% yield.

Imine Formation Step. The last stage of imine formation in coupling with HBP vector was initially carried out in water, the only solvent compatible with the vector.[61] However, multiple attempts to reproduce this approach, especially during scale-up, produced a modest 32% average yield, lower than expected. Our current study, however, revealed Vector's remarkable solubility in 1−5% TFA in DMSO, which allowed a twofold raise in the reaction yield, improving reproducibility and ensuring scalability in the final step. Subsequently, the final product was neutralized and purified on C_{18} column, ensuring the best purity. Obtained as a highly water-soluble sodium-neutral salt, compound 1102−39 allowed a detailed exploration of its physicochemical and biological properties.

Earlier we reported a glycol hydrazide analogue **8** of the 1102−39 compound[61] (Figure 3). It lacked an aromatic cycle

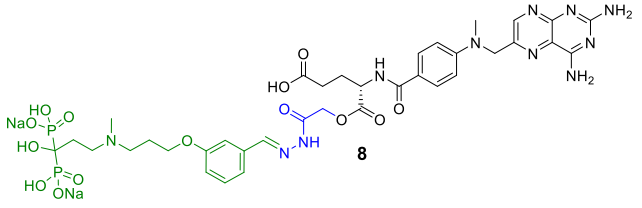

Figure 3. Glycol hydrazide analogue of the 1102−39.

in its linker part and was obtained by using the same scheme. However, its stability during production was lower, possibly due to intramolecular cyclization within the linker fragment.

Structure. In certain cases, MTX substitution remains hypothetical in the literature or is only indirectly linked to the physicochemical properties. On the contrary, certain studies have definitively confirmed substitution through the complete synthesis of the MTX moiety, starting from partially protected glutamic acid.[110] We found a convenient way to prove the structure of the resulting 1102−39 compound through a 2D NMR HMBC experiment, which allows the

https://doi.org/10.1021/acsomega.4c06029
ACS Omega 2024, 9, 42433−42447

determination of the atomic environment for each MTX carboxylic group. Key HMBC correlations are depicted in the Figure 4.

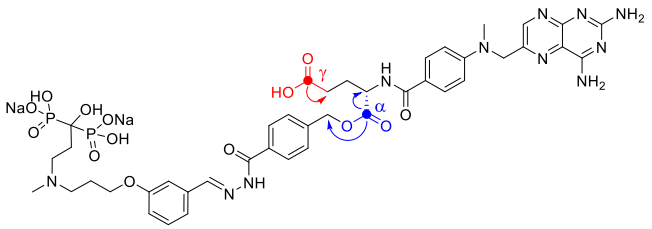

Figure 4. Key HMBC correlations proving the 1102−39 molecule structure.

Binding of 1102−39 to Hydroxyapatite (HA). Mineral binding is crucial for drug retention in bone.[72] In a biodistribution study of the MTX-BP conjugate,[75] roughly 20% of the administered dose accumulated in mouse skeletal tissue was observed and was comparable to BP-vector alone.[85] The in vitro tests performed at RT demonstrated rapid (within 30 min) and high binding of 1102−39 to HA around 92% (Figure 5).

MTX release from the 1102−39 molecule fixed on HA under DPBS (varying pH 7.4 and 6.4) and in a cell conditioned medium (pH around 7.0). While the ester group can effectively release the active molecule,[36,48] the cleavage must be confirmed,[74] as sometimes the ester group can be stable.[51,54,55] The gradual release of MTX from the hydroxyapatite-fixed 1102−39 was confirmed by comparison with the native MTX HPLC-UV profile. The MTX release from the HA-fixed molecule in DPBS (pH 7.4 and 6.4) and in a cell-conditioned medium (pH around 7.0) was quite similar: 10% over a period of 461 h (approximately 1% per 24 h period) (Figure 5).

Stability of 1102−39 in a DPBS Solution Stored at Room Temperature (RT). Based on measured HPLC-UV purity at 308 nm, 1102−39 in Dulbecco's phosphate-buffered saline (DPBS) (pH 7.4) solution stored at RT is stable at least 24 h (purity >90%) with a degradation process reaching around 10% over a period of approximately 70 h (Figure 6).

If the cleavage rate is optimal, it will be determined through in vivo testing, as this parameter is molecule specific. The local pathological microenvironment (pH, enzymes) may accelerate the cleavage rate, but even passive hydrolysis may be sufficient if its rate remains lower than the short transport time to the bone site.[30,54]

In Vitro Cytotoxic Activity of the 1102−39 Compound. In vitro evaluations of 1102−39 (HBP-MTX) as well as native MTX were conducted through several studies on multiple cell lines as presented on Figure 7.

These in vitro studies confirmed the prodrug nature of 1102−39 by demonstrating its 10-fold lower cytotoxicity compared to that of MTX, which aligns with typical in vitro behavior for prodrug molecules (IC50 = 10−50 nM for MTX and 100−500 nM for 1102−39).

This reduction in activity correlates with the API release capacity.[36,44] A similar decrease in in vitro activity was observed for Camdronate (camptothecin-ester-BP),[36] the 12B80 molecule (HBP-vectorized doxorubicin)[65] and the 18A184 prodrug (NSAID HBP-meloxicam),[67] which exhibited substantial activity in rodents and dogs.[65,67,78] Based on this profile, the 1102−39 molecule appears well-matched for in vivo applications.

In vivo toxicity: determination of the maximal tolerated dose (MTD) in rats and mice for 1102−39 administered per IV route. The MTD was evaluated in vivo in male mice after repeated IV administration (Figures 8 and 9).

Body weight was monitored and expressed as percentage body weight gain versus Day 0 following repeated while increasing dose IV injection of 1102−39 on D0, D7, D13, and D20 in C57BL6 mice (n = 1 mouse administered per treatment regimen type).

Body weight (mean ± SD, n = 3 per time point) was monitored following repeated IV injection of 1102−39 on Swiss mice at D0, D7, D14, D18, and D24.

1102−39 was well tolerated in mice up to 104 mg/kg and up to 31.2 mg/kg in repeated administration once a week over 5 weeks.

The MTD was evaluated in vivo in male rat after repeated IV administration (Figure 10).

Preliminary studies showed that a single IV administration of 1102−39 above 10.4 mg/kg (i.e., 20.8 and 31.2 mg/kg) was not tolerated in male Sprague−Dawley rats (data not shown).

Body weight was monitored and expressed as percentage body weight gain versus Day 0 following repeated IV injection of 1102−39 on D0, D7, and D14 in Sprague−Dawley rats (1 rat per tested condition).

1102−39 was well tolerated in rats up to 10.4 mg/kg following single IV administration (data not shown) and up to 5.2 mg/kg in repeated administration once a week over 3 weeks.

In Vivo Efficacy of 1102−39 in Osteosarcoma Model in Mice. Efficacy of treatment with repeated injections of 1102−39 was evaluated in the LM8 osteosarcoma model. Mice were injected weekly with 1102−39 (20 mg/kg) for three consecutive weeks. Antitumor efficacy of 1102−39 was correlated to injection cumulative dose, with an increase of efficacy from D13, D20, D27, and D34 (Figure 11A). Survival at 34 days was identical in both groups (90%). Treatment with 1102−39 reduced tumor volume by 44% compared to DPBS vehicle-treated mice but did not achieve statistical significance primarily due to the high variability of tumor growth in the untreated group. Nevertheless, at euthanasia (D34) tumor weight (Figure 11B) in the 1102−39 treated group (mean: 1.2 g/SD: 0.6 g/median: 1.2 g/range [0.4−2.5]) statistically differs from control group (mean: 2.9 g/SD: 2.4 g/median: 1.8 g/range [0.8−6.4]. In addition, the para osseous LM8 osteosarcoma model has the characteristic to easily metastasize in soft tissues. 1102−39 slightly decreased metastatic cells observed in lungs (44%), kidneys (33%), and liver (11%) versus in the lungs (50%), kidneys (40%), and liver (20%) in the DPBS control group.

CONCLUSIONS

The 1102−39 consists of three building blocks: the methotrexate bound by the linker to the bone targeted HBP Vector through imine bonds. The innovation was based on a hydroxybisphosphonate methotrexate prodrug using a cleavable ester-releasing group. Developed approach led to a reliable synthesis, doubling the overall yield of the 1102−39 compound and increasing purification efficiency and synthesis scalability. The prodrug nature of 1102−39 was demonstrated through cytotoxicity tests performed on various established cell lines and a progressive release of methotrexate. Additionally, it

https://doi.org/10.1021/acsomega.4c06029
ACS Omega 2024, 9, 42433−42447

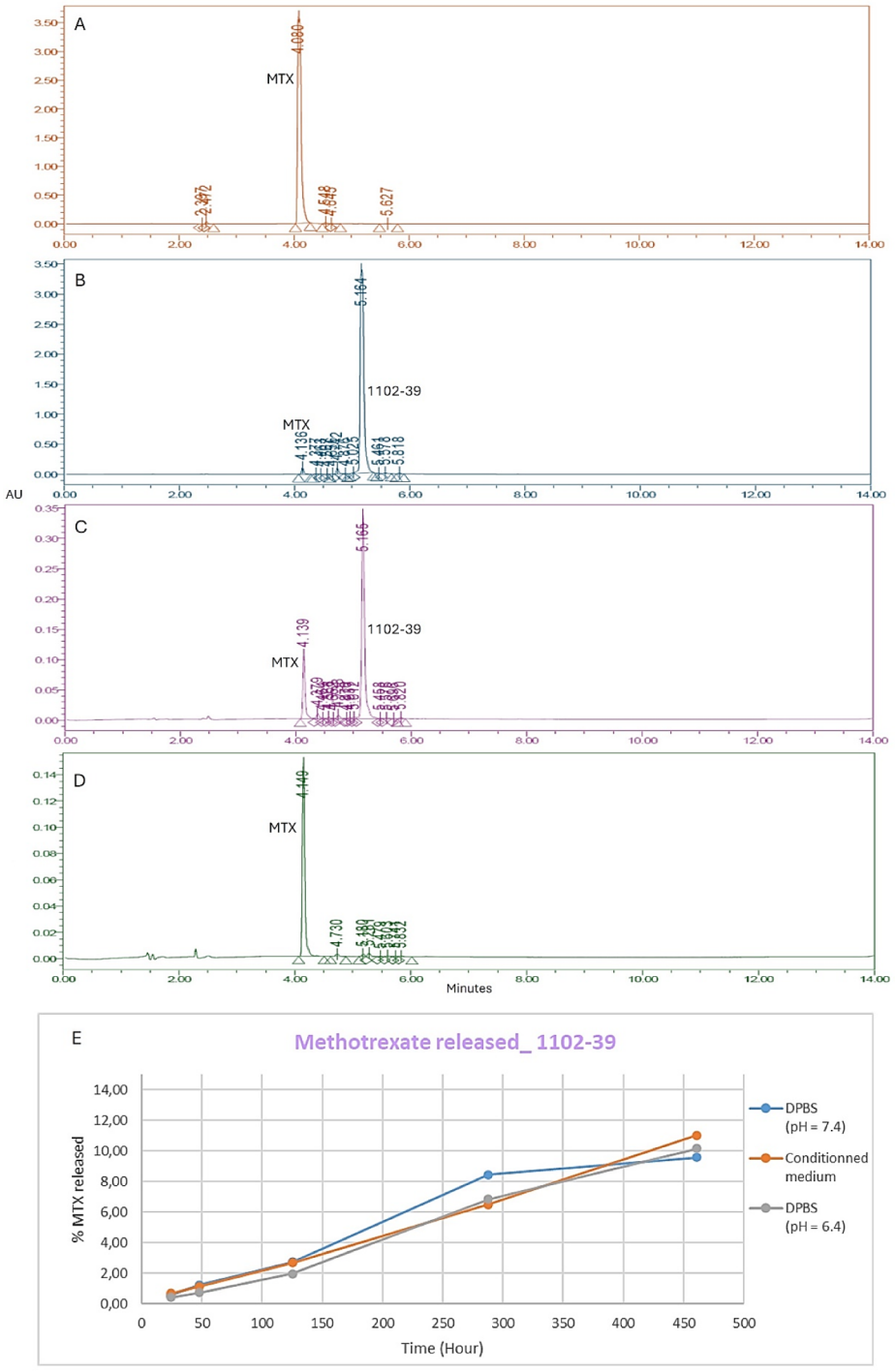

Figure 5. Determination of MTX release from HA-bound 1102−39 by HPLC-UV at 308 nm. **A**: HPLC-UV chromatogram of methotrexate; **B**: HPLC-UV chromatogram of 1102−39; **C**: HPLC-UV chromatogram of the remaining solution after 30 min of 1102−39 fixation on HA reveals residual product in solution, confirming HA saturation; **D**: HPLC-UV chromatogram of methotrexate gradual liberation from 1102-39-HA (T = 288 h, DPBS); **E**: release of methotrexate from saturated HA with 1102−39 investigated by HPLC-UV in DBPS at two pH (6.4 and 7.4) and in conditioned medium (prepared using medium from cells that have been grown with a minimum of 80% confluency and without medium replacement for three consecutive days).

exhibited high affinity for hydroxyapatite and a good stability in solution at ambient temperature. 1102−39 (20.8 mg/kg) promoted important antitumor effects on mice orthotopic osteosarcoma while slightly reducing metastasis in soft tissues (lungs, kidneys, liver) and significantly decreasing the tumor weight at euthanasia (D34). These findings make the 1102−39 substance suitable for upcoming studies, and its profile looks promising for other in vivo treatments specific to the osteoarticular system in the therapy of tumor and inflammation diseases. Furthermore, the developed chemical methodology makes more efficient the development of new HBP-vectorized therapeutic prodrugs.

https://doi.org/10.1021/acsomega.4c06029
ACS Omega 2024, 9, 42433−42447

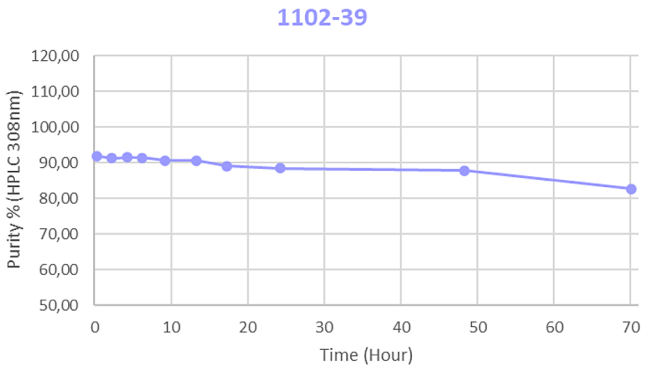

Figure 6. Stability of 1102−39 in solution in DPBS over a period of 70 h.

EXPERIMENTAL PROCEDURES

Synthesis. *Compound 3.* The mixture of phenol **1** (169 mg, 1.8 mmol, 1 equiv) and 4-bromomethyl benzoyl bromide **2** (500 mg, 1.8 mmol, 1 equiv) was fused and agitated at 90 °C under reduced pressure during 20 min. After cooling, the crystalline solid **3** was obtained, 520 mg, yield 99%. ^{1}H NMR ($CDCl_3$, 400 MHz): δ 8.21 (d, 2H), 7.56 (d, 2H), 7.46 (t, 2H), 7.31 (t, 1H), 7.24 (d, 2H), 4.56 (s, 2H). Additional details are provided in the Supporting Information.

Compound 5. DMF (6 mL) was added to the mixture of methotrexate (**4**) (600 mg, 1.32 mmol, 1 equiv), **3** (460 mg, 1.58 mmol, 1.2 equiv) and Na_2CO_3 (140 mg, 1.32 mmol, 1 equiv) and the resulting mixture was stirred during 16 h at RT. The reaction mixture was directly purified on silica gel column in gradient DCM/Et_2O = 1/1 → DCM/Et_2O/MeOH = 1/1/2, TLC: DCM/Et_2O/MeOH = 2/6/1. The solvent was removed under reduced pressure, and pure **5** was obtained, 327 mg of yellow solid, yield 37%. MS: $[M + H]^+$ m/z = 665.7.

Figure 7. Assessment of the cytotoxicity of 1102−39 compared to MTX in viability assays conducted on established cell lines. K7M2: osteoblast from the bone of a mouse with osteosarcoma; L929: mouse fibroblasts; LM8: mouse osteosarcoma; OSRGa: rat osteosarcoma; SaOS2: human osteosarcoma; TC-71: human Ewing's sarcoma.

https://doi.org/10.1021/acsomega.4c06029
ACS Omega 2024, 9, 42433−42447

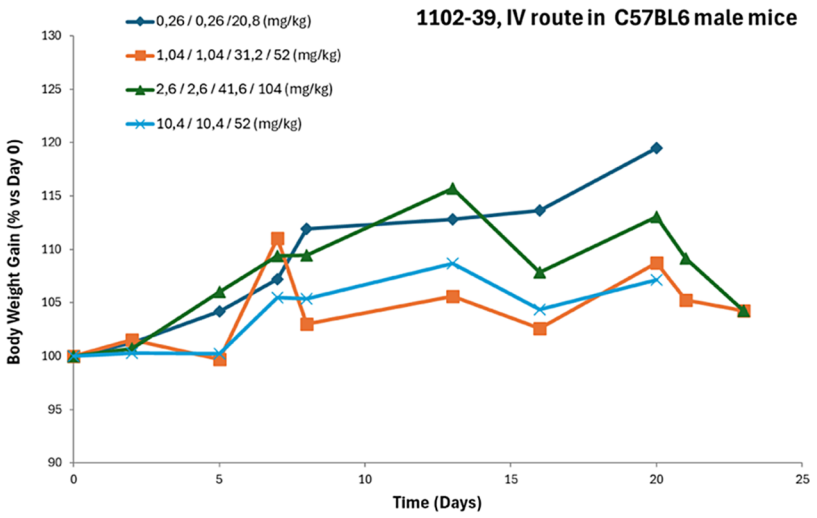

Figure 8. Systemic toxicity of repeated administrations while increasing the dose of 1102−39 on the body weight of C57BL6 male mice.

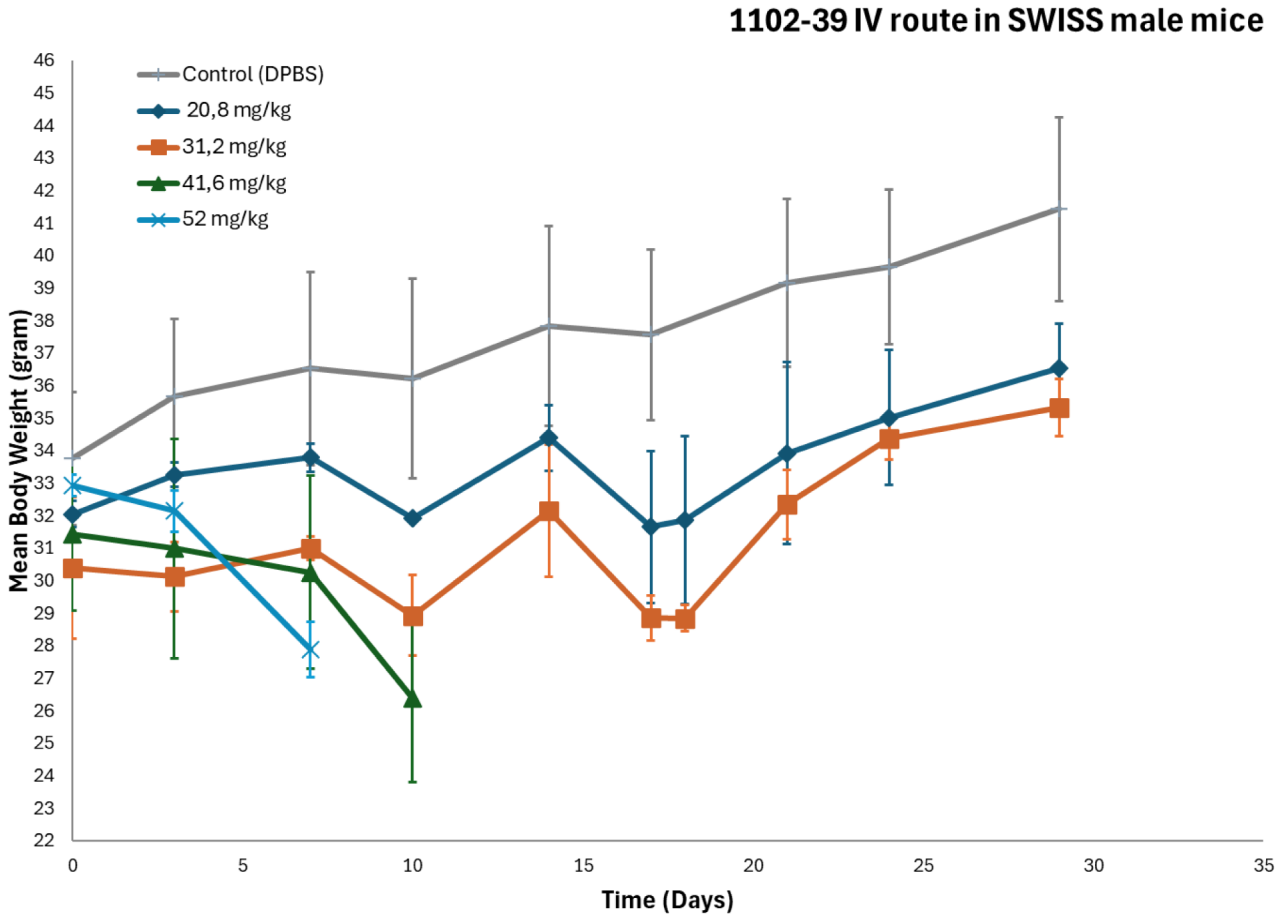

Figure 9. Systemic toxicity of repeated administrations of 1102−39 on the body weight of SWISS male mice.

^{1}H NMR (CDCl3-MeOD, 400 MHz): δ 8.31 (s, 1H), 7.90 (d, 2H), 7.49 (d, 2H), 7.24 (2H), 7.17 (t, 2H), 7.02 (t, 1H), 6.93 (d, 2H), 6.53 (d, 2H), 5.02 (s, 2H), 4.54 (s, 2H), 4.46 (m, 1H), 2.96 (s, 3H), 2.18 (t, 2H), 2.03 (m, 1H), 1.89 (m, 1H). Additional details are provided in the Supporting Information.

Compound 6. Hydrazine hydrate (1 M in THF, 1.54 mL, 1.15 equiv) was added to the solution of **5** (890 mg, 1.34 mmol, 1 equiv) in the mixture of DCM (54 mL) and MeOH (14 mL) under stirring and all the solution was evaporated at 40 °C under reduced pressure, and at the moment, when the last quantity of the solvent disappears completely, the mixture of hydrazine hydrate (1 M in THF, 1.54 mL, 1.15 equiv), DCM (54 mL), and MeOH (14 mL) was added and all the solution was evaporated at 40 °C under reduced pressure until the moment, when the last quantity of the solvent disappears completely, when THF (5 mL) was added at RT followed by the water (3 mL) under sonication until the transparent solution formation. Then MeOH (50 mL) was added gradually

https://doi.org/10.1021/acsomega.4c06029
ACS Omega 2024, 9, 42433−42447

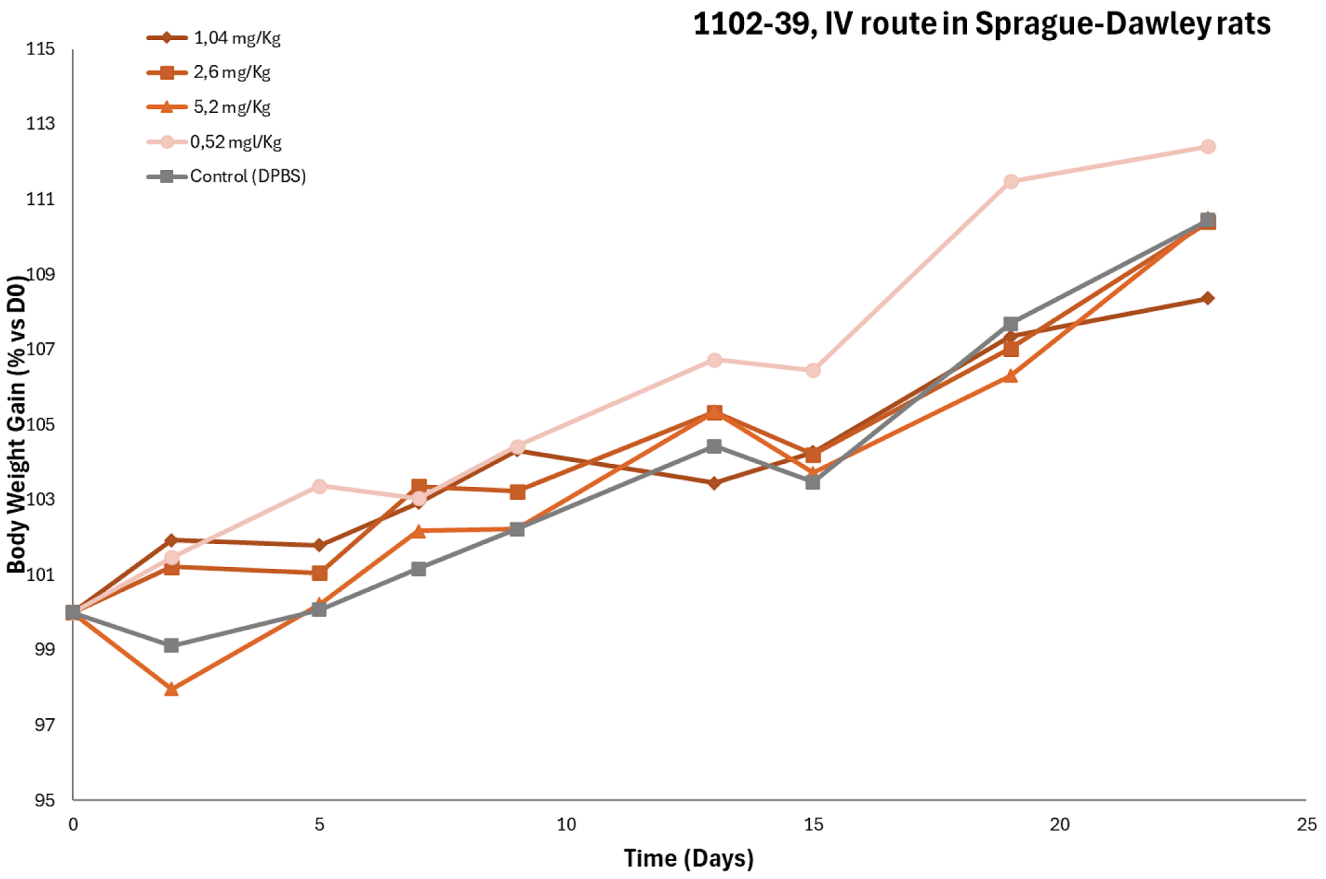

Figure 10. Systemic toxicity of repeated administrations of 1102−39 on the body weight of Sprague−Dawley male rats.

with agitation resulting in the solid formation. Ether (125 mL) was added gradually with agitation and after 5 min of stirring at RT the solid was filtered, washed with ether and dried under reduced pressure. The **6** was obtained, 710 mg of yellow powder, yield 88%. MS: $[M + H]^+$ m/z = 603.8. ^{1}H NMR (MeOD, 400 MHz): δ 8.60 (s, 1H), 7.69 (m, 4H), 7.46 (d, 2H), 6.88 (d, 2H), 5.27 (d, 1H), 5.23 (d, 1H), 4.83 (s, 2H), 4.50 (dd, 1H), 3.22 (s, 3H), 2.31 (m, 2H), 2.19 (m, 1H), 2.10 (m, 1H). Additional details are provided in the Supporting Information.

Compound 1102−39. Vector (7) (132 mg, 0.29 mmol, 1.3 equiv) and **6** (132 mg, 0.22 mmol, 1 equiv) were solubilized in 1%TFA/DMSO (6.6 mL) gently heating up to 60 °C if necessary. After 15 min, the reaction mixture was diluted with 0.5 M $NaHCO_3$ (130 mL) under stirring at RT and filtered. The obtained yellow solution was introduced in C18 column and eluted in gradient: 3% MeOH → 30% MeOH. The pure fractions were concentrated at reduced pressure at 25−35 °C up to 5 mL and diluted under agitation with MeOH (50 mL) followed by Et_2O (250 mL), and the precipitate was filtered and dried under reduced to give pure 1102−39, 140 mg, yield 62%. MS: $[M + H]^+$ m/z = 996.6. ^{1}H NMR (5%TFA-D/DMSO−D6, 400 MHz): δ 8.72 (s, 1H), 8.43 (s, 1H), 7.90 (d, 2H), 7.76 (d, 2H), 7.50 (d, 2H), 7.36 (m, 2H), 7.03 (d, 1H), 6.83 (d, 2H), 5.21 (s, 2H), 4.87 (s, 2H), 4.48 (dd, 1H), 4.13 (br tr, 2H), 3.57−3.24 (m, 4H), 3.24 (s, 3H), 2.83 (s, 3H), 2.38−2.22 (m, 4H), 2.15 (m, 3H), 2.00 (m, 1H). ^{31}P NMR (5%TFA-D/DMSO−D_6, 162 MHz): δ 18.06 (t). Additional details, including the ^{13}C NMR spectrum, are provided in the Supporting Information.

Safety. As for cytotoxic agents, methotrexate and 1102−39 were handled with care using gloves, masks, lab coats, and glasses for solutions and under chemical fume hood in addition for powder.

Physicochemical Characterization. Flash chromatography purification was conducted using a Gilson PLC2020 system and C18 cartridges from Macherey Nagel. Thin layer chromatography (TLC) was performed on Merck Silica Gel 60 F254 plates, and the developed plates were visualized under a UV lamp at 254 nm. NMR spectra were recorded at 400 MHz for ^{1}H, 101 MHz for ^{13}C and 162 MHz for ^{31}P at 303 K on samples dissolved in the appropriate deuterated solvent. Used references were the deuterated solvent signal for residual ^{1}H. Chemical displacement values (δ) are expressed in parts per million (ppm), and coupling constants (J) are in hertz (Hz). HPLC-UV studies were conducted using Waters system with a Phenomenex Luna Column 5u C18(2) 100 Å 150 × 4.6 mm. Chromatographic conditions were as follows: flow 1.0 mL/min; mobile phase A—ammonium acetate 20 mM and 0.02% $EDTANa_2$ and NH_4OH (pH = 8.7), B—acetonitrile, injection volume 20 μL; gradient, initial mobile phase 5% B, 0−10 min increased to 70%, 10−12 min 70%B, 12−14 min decreased to initial mobile phase. UV detection was performed at a wavelength of 308 nm. All reagents were purchased from Sigma-Aldrich or TCI and were used as supplied by the manufacturer.

The Binding Efficiency of the 1102−39 Molecule to Hydroxyapatite (HA). Hydroxyapatite was purchased from Biorad. The solution of 1102−39 molecule in DPBS (1 mg/mL (i.e 0.96 mM)) was added to HA powder (50 mg). The

https://doi.org/10.1021/acsomega.4c06029
ACS Omega 2024, 9, 42433−42447

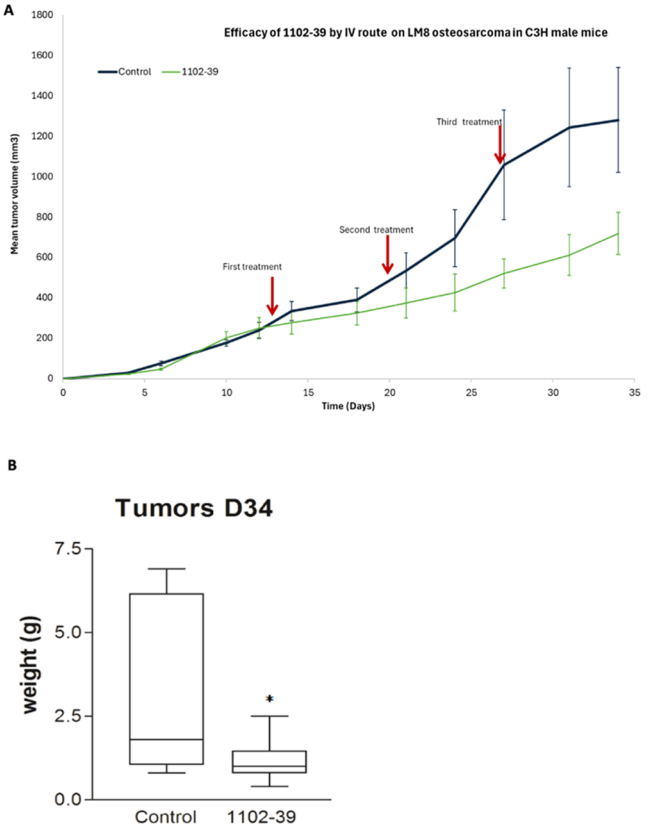

Figure 11. 1102−39 efficacy in mice measurement of the tumor volume (mm^3). **A**: 1102−39 treatment reduced tumor growth in the osteosarcoma model over time. Orthotopic paratibial LM8 tumors were implanted on D0 in C3H mice and IV treatment with 1102−39 or DPBS vehicle were administered every week for 3 weeks from D13. n = 10 mice per group. Mean ± SEM **B**: 1102−39 was potent in inhibiting terminal osteosarcoma tumor weight. Orthotopic paratibial LM8 tumors were implanted in C3H mice. Mice received IV treatment with DPBS vehicle or 1102−39 on D13, D20 and D27. n = 9 mice per group. Statistical analysis on D34: Mann−Whitney test. * $p < 0.05$.

obtained mixture was agitated on a rotary shaker for 30 min at RT. Subsequently, the supernatant was collected and the powder was washed twice with DPBS (5 mL each), followed by filtration. The powder was further washed with ethanol and dried under reduced pressure. The supernatant was collected, stored at −20 °C and analyzed by HPLC-UV at 308 nm to determine the concentration from % area using a calibration curve and then to calculate the rate of binding (difference between the initial concentration of 0.96 mM and the final concentration of unbound molecule in the supernatant): the binding rate was set at 92.2%.

MTX Release from 1102-39 Molecule Fixed on HA under pH 6.4, 7.4, and Conditioned Medium (pH 7.0). The MTX release was evaluated in DPBS (pH 7.4 and pH 6.4) and a conditioned medium on HA-fixed 1102−39. Conditioned medium was prepared by using medium from cells grown to a minimum of 80% confluency without medium replacement for 3 days and separated from the cells by centrifugation at 2000 g for 10 min. The supernatant (conditioned medium) was stored at +4 °C until beginning of the test. Five mg of HA-bound BP-MTX powder was placed into a Greiner tissue culture 24-well plate with Transwell inserts of 0.4 μm pore size, translucent PET membrane. 500 μL of liquid (medium or DPBS) was added and incubated at +37 °C. Analyses were performed by collecting 20 μL of medium or DPBS replaced by 20 μL of medium or DPBS at 24, 48, 125, 288, and 461 h in triplicate by HPLC-UV at 308 nm.

Cell Line. The established cell lines K7M2 (osteoblast from the bone of a mouse with osteosarcoma), LM8 (mouse osteosarcoma), OSRGa (rat initially radioinduced osteosarcoma), and SaOS2 (human osteosarcoma) were grown in DMEM cell culture medium supplemented with 10% fetal bovine serum in a humidified 5% CO2 chamber at +37 °C. L929 (mouse fibroblasts) and TC-71 (human Ewing's sarcoma) cells were grown in RPMI cell culture medium supplemented with 10% fetal bovine serum in a humidified 5% CO2 chamber at +37 °C.

Cell Viability Assay. Cell viability was quantified by measuring metabolic activity with the WST-1 assay (Roche). Briefly, cells were plated into 96-well-plates at an initial density of 2000 cells/well (OSRGa and TC71), 1500 cells/well (K7M2, SaOS2, and LM8) and 1000 cells/well (L929). Cells were grown in a humidified 5% CO2 chamber at +37 °C in their respective cell culture media (RMPI or DMEM supplemented with 10% FBS). After 24 h, cells were treated for 72 h with methotrexate (dissolved in DPBS added with 1% Na_2CO_3) or with 1102−39 (dissolved in DPBS) at concentrations ranging from 5 nM to 50 μM, or with their respective control solvent. Cell viability was assessed after 72 h by measuring the reduction of tetrazolium salt WST-1 to formazan at +37 °C. Absorbance of the reduction reaction was read at 420 and 480 nm with a microplate reader (Multiskan Go, 5111 9200, Thermofisher). Measure was stopped when the absorbance of solvent treated cells reached a value between 1.5 and 2. The mean optical density (OD, absorbance) of three wells in the indicated treated condition was used to calculate the percentage of cell viability as follows: percentage of cell viability = (Atreatment − Ablank)/(Acontrol − Ablank) × 100% (where A = absorbance) ± standard deviation (SD) expressed in %.

Animals. All procedures and experimental protocols used were in compliance with the 2010/63/EU directive of the European Parliament for the protection of animals used for scientific purposes. All experiments were approved by the French Research Ministry (project authorization MESR#01489.01) and were in accordance with the institutional guidelines of the Regional Ethical Committee for animal experiment (CEEA PdL06). Mice and rats were purchased from Janvier Laboratories and were acclimatized for a minimum of 7 days prior to the beginning of the study; 5- to 6-week-old male Swiss mice, C3H or male C57BL/6, and 12-week-old male Sprague−Dawley rats were included in protocols. All animals were housed in pathogen-free and controlled conditions (temperature 22 ± 2 °C, humidity 55 ± 10%) on a 12 h light-dark cycle, in cages of 3 to 5 animals. All animals had free access to 0.2 μm of filtered water and were fed ad libitum with a commercial chow. Animals were identified by individual ear tags and monitored every day for their clinical status. As a general measure of gross toxicity, body weight monitoring was performed twice a week. Euthanasia was performed by cervical dislocation under isoflurane inhalation anesthesia.

Treatment of Rodents. 1102−39 powder was solubilized in DPBS. Male mice and rats were treated once a week with intravenous bolus injection of 1102−39 in the tail vein (as

https://doi.org/10.1021/acsomega.4c06029
ACS Omega 2024, 9, 42433−42447

slowly as possible) using a 29G insulin syringe at 1 up to 10 mL/kg (mice) and 0.5 up to 5 mL/kg (rats).

For MTD evaluation with repeated while increasing dose, C57BL6 mice (6 weeks old at treatment start) were treated with 1102−39 (0.26−104 mg/kg) on D0, D7, D13, or D20 and were euthanized on D20 or D23.

For MTD evaluation with repeated doses, Swiss mice (5 weeks old at treatment start) were treated with 1102−39 (20.8 up to 52 mg/kg) or with DPBS (vehicle control group) on D0, D7, D14, D18, and D24 and were euthanized on D29 at the latest.

For MTD evaluation with repeated doses, Sprague−Dawley rats (12 weeks old at treatment start) were treated with 1102−39 (0.52 up to 31.2 mg/kg) or with DPBS (vehicle control group) on D0, D7, and D14 and were euthanized on D23.

For antitumor efficacy, LM8 tumors were inoculated on CH3 mice (5 weeks old on D0), mice (7 weeks old) received injection of 1102−39 (20.8 mg/kg (20 μmol/kg), volume rate 10 mL/kg) once a week for 3 weeks (on D13, D20, and D27) and were euthanized on D34 (7 days post last dosing).

Experimental Osteosarcoma Model. Osteosarcoma model was induced by injection of LM8 mouse osteosarcoma cell line to male C3H mice. Two $\times 10^6$ cells in 15 μL of DPBS were injected in close contact with the right tibia, after light periost scratching, on mice anesthetized by isoflurane inhalation (air 0.5 L/min and isoflurane 2%). Tumor volume was quantified twice a week by measuring two perpendicular diameters with a Vernier caliper and calculated with the formula: (l^2 x L)/2 (l, the smallest, and L, the largest diameter). Based on our historical data at Atlanthera, this experimental mouse model of osteosarcoma showed an incidence of 90% for the development of a mineralized tumor mass which can be measured from Day 8 and reached a volume of 500−800 mm^3 on D34, with lung and liver metastases; 90% of tumors were measurable (on D12) and randomly distributed between control and 1102−39 treated group. Mice with tumor volume below 50 mm^3 on randomization day were excluded from protocol. Mice with tumor volumes exceeding 2500 mm^3 were sacrificed.

Statistical Methods. In vitro cell viability studies were performed in triplicate and presented as mean ± SD. In vivo studies of MTD were conducted on 1 or 3 animals per group and time point; body weight was presented in mean ± SD, but no analysis was performed on these small samples. In vivo studies of efficacy were conducted on 10 mice per group and tumor volumes were presented as mean ± SEM. Statistical analysis was presented for the terminal weight of the tumor at D34, by Mann−Whitney test. Statistical analysis was performed using Prism and Excel software's. Probability values of less than 0.05 (two-tailed) were used as the critical level of significance. Mean values were annotated with an asterisk symbol (*p-value <0.05).

■ ASSOCIATED CONTENT

Supporting Information

The Supporting Information is available free of charge at https://pubs.acs.org/doi/10.1021/acsomega.4c06029.

NMR and MS spectra; IUPAC name of 1102−39 molecule (PDF)

■ AUTHOR INFORMATION

Corresponding Author

Maxim Egorov − *Atlanthera, Saint-Herblain 44821, France;* orcid.org/0009-0008-2007-7191; Email: Maxim.Egorov@atlanthera.com

Authors

Jean-Yves Goujon − *Atlanthera, Saint-Herblain 44821, France*

Marie Sicard − *Atlanthera, Saint-Herblain 44821, France*

Christelle Moal − *Atlanthera, Saint-Herblain 44821, France*

Samuel Pairel − *Atlanthera, Saint-Herblain 44821, France*

Ronan Le Bot − *Atlanthera, Saint-Herblain 44821, France*

Complete contact information is available at: https://pubs.acs.org/10.1021/acsomega.4c06029

Author Contributions

R.L. Bot conceived and lead the project. M.E. designed and carried out the synthetic and purification work. J.-Y.G. carried out hydroxyapatite and stability tests of 1102−39 using an HPLC-UV method. In vitro and in vivo experiments were carried out by M.S., C.M., and S.P. M.E. wrote this paper.

Notes

The authors declare no competing financial interest.

■ ACKNOWLEDGMENTS

We sincerely thank Dr. Viviane Bertrand from Atlanthera for her constructive feedback, rigor, and thoughtful suggestions in the preparation of this manuscript, especially in the analysis of biological data. Her contributions have greatly supported our research.

■ ABBREVIATIONS

BP, bisphosphonate; D, day; DPBS, dulbecco's phosphate buffer saline; HA, hydroxyapatite; HBP, hydroxybiphosphonate; IC50, half maximal inhibitory concentration; MTD, maximum tolerated dose; MTX, methotrexate; NSAID, non-steroidal anti-inflammatory drug

■ REFERENCES

(1) Huennekens, F. M. The Methotrexate Story: A Paradigm for Development of Cancer Chemotherapeutic Agents. *Adv. Enzyme Regul.* **1994**, *34*, 397−419.

(2) Abolmaali, S. S.; Tamaddon, A. M.; Dinarvand, R. A review of therapeutic challenges and achievements of methotrexate delivery systems for cancer and rheumatoid arthritis treatment. *Cancer Chemother. Pharmacol.* **2013**, *71* (5), 1115−1130.

(3) Shin, J. M.; Kim, S.-H.; Thambi, T.; You, D. G.; Jeon, J.; Lee, J. O.; Chung, B. Y.; Jo, D.-G.; Park, J. H. A hyaluronic acid−methotrexate conjugate for targeted therapy of rheumatoid arthritis. *Chem. Commun.* **2014**, *50* (57), 7632−7635.

(4) Peiró Cadahía, J.; Bondebjerg, J.; Hansen, C. A.; Previtali, V.; Hansen, A. E.; Andresen, T. L.; Clausen, M. H. Synthesis and Evaluation of Hydrogen Peroxide Sensitive Prodrugs of Methotrexate and Aminopterin for the Treatment of Rheumatoid Arthritis. *J. Med. Chem.* **2018**, *61* (8), 3503−3515.

(5) Brugières, L.; Piperno-Neumann, S. La chimiothérapie des ostéosarcomes. *Oncologie* **2007**, *9*, 164−169.

(6) Egan, L. J.; Sandborn, W. J. Methotrexate for Inflammatory Bowel Disease: Pharmacology and Preliminary Results. *Mayo Clin. Proc.* **1996**, *71* (1), 69−80.

(7) Letendre, P. W.; DeJong, D. J.; Miller, D. R. The Use of Methotrexate in Rheumatoid Arthritis. *Drug Intell. Clin. Pharm.* **1985**, *19* (5), 349−358.

(8) Garcia, L. D.; Gibson, L.; Lambert, W.; Li, B. W.; Zhu, L. Sustained release formulation of methotrexate as a disease-modifying antirheumatic drug (DMARD) and an anti-cancer agent. US2011280932A1, 2011.
(9) Wang, Y.; Jones, G.; Keen, H. I.; Hill, C. L.; Wluka, A. E.; Kasza, J.; Teichtahl, A. J.; Antony, B.; O'Sullivan, R.; Cicuttini, F. M. Methotrexate to treat hand osteoarthritis with synovitis (METH-ODS): an Australian, multisite, parallel-group, double-blind, randomised, placebo-controlled trial. *Lancet* **2023**, *402* (10414), 1764−1772.
(10) Mathieu, S.; Tournadre, A.; Soubrier, M.; Sellam, J. Effect of disease-modifying anti-rheumatic drugs in osteoarthritis: A meta-analysis. *Jt., Bone, Spine* **2022**, *89* (6), 105444.
(11) Jain, S.; Mathur, R.; Das, M.; Swarnakar, N. K.; Mishra, A. K. Synthesis, pharmacoscintigraphic evaluation and antitumor efficacy of methotrexate-loaded, folate-conjugated, stealth albumin nanoparticles. *Nanomedicine (Lond.)* **2011**, *6* (10), 1733−1754.
(12) Böhme, D.; Beck-Sickinger, A. G. Controlling Toxicity of Peptide−Drug Conjugates by Different Chemical Linker Structures. *ChemMedchem* **2015**, *10*, 804−814.
(13) Stehle, G.; Sinn, H.; Wunder, A.; Schrenk, H. H.; Schütt, S.; Maier-Borst, W.; Heene, D. L. The loading rate determines tumor targeting properties of methotrexate-albumin conjugates in rats. *Anticancer Drugs* **1997**, *8* (7), 667−685.
(14) Warnecke, A.; Fichtner, I.; Sass, G.; Kratz, F. Synthesis, cleavage profile, and antitumor efficacy of an albumin-binding prodrug of methotrexate that is cleaved by plasmin and cathepsin B. *Arch. Pharm. (Weinheim)* **2007**, *340* (8), 389−395.
(15) Kaasgaard, T.; Andresen, T. L.; Jensen, S. S.; Holte, R. O.; Jensen, L. T.; Jørgensen, K. Liposomes containing alkylated methotrexate analogues for phospholipase A(2) mediated tumor targeted drug delivery. *Chem. Phys. Lipids* **2009**, *157* (2), 94−103.
(16) Wang, Y.; Yang, X.; Yang, J.; Wang, Y.; Chen, R.; Wu, J.; Liu, Y.; Zhang, N. Self-assembled nanoparticles of methotrexate conjugated O-carboxymethyl chitosan: Preparation, characterization and drug release behavior *in vitro*. *Carbohydr. Polym.* **2011**, *86* (4), 1665−1670.
(17) Li, M. H.; Choi, S. K.; Thomas, T. P.; Desai, A.; Lee, K. H.; Kotlyar, A.; Banaszak Holl, M. M.; Baker, J. R., Jr. Dendrimer-based multivalent methotrexates as dual acting nanoconjugates for cancer cell targeting. *Eur. J. Med. Chem.* **2012**, *47* (1), 560−572.
(18) Mitxelena-Iribarren, O.; Hisey, C. L.; Errazquin-Irigoyen, M.; González-Fernández, Y.; Imbuluzqueta, E.; Mujika, M.; Blanco-Prieto, M. J.; Arana, S. Effectiveness of nanoencapsulated methotrexate against osteosarcoma cells: *in vitro* cytotoxicity under dynamic conditions. *Biomed. Microdevices* **2017**, *19* (2), 35.
(19) Ferreira, M.; Chaves, L. L.; Lima, S. A.; Reis, S. Optimization of nanostructured lipid carriers loaded with methotrexate: A tool for inflammatory and cancer therapy. *Int. J. Pharm.* **2015**, *492* (1−2), 65−72.
(20) Riebeseel, K.; Biedermann, E.; Löser, R.; Breiter, N.; Hanselmann, R.; Mülhaupt, R.; Unger, C.; Kratz, F. Polyethylene glycol conjugates of methotrexate varying in their molecular weight from MW 750 to MW 40000: synthesis, characterization, and structure-activity relationships *in vitro* and *in vivo*. *Bioconjugate Chem.* **2002**, *13* (4), 773−785.
(21) Nagy, A.; Szoke, B.; Schally, A. V. Selective coupling of methotrexate to peptide hormone carriers through a γ-carboxamide linkage of its glutamic acid moiety: benzotriazol-1-yloxytris-(dimethylamino)phosphonium hexafluorophosphate activation in salt coupling. *Proc. Natl. Acad. Sci. U. S. A.* **1993**, *90* (13), 6373−6376.
(22) Böhme, D.; Krieghoff, J.; Beck-Sickinger, A. G. Double Methotrexate-Modified Neuropeptide Y Analogues Express Increased Toxicity and Overcome Drug Resistance in Breast Cancer Cells. *J. Med. Chem.* **2016**, *59* (7), 3409−3417.
(23) Li, Y.; Lin, J.; Liu, G.; Ma, J.; Xie, L.; Guo, F.; Zhu, X.; Hou, Z. Dual-acting, function-responsive, and high drug payload nanospheres for combining simplicity and efficacy in both self-targeted multi-drug co-delivery and synergistic anticancer effect. *Int. J. Pharm.* **2016**, *512* (1), 194−203.
(24) Senderikhin, A.; Ayalon, O.; Shapiro, I.; Vinnikova, M.; Kozak, A.; Ershov, L. Phospholipid prodrugs of anti-proliferative drugs. WO 0119320 A2, 2001.
(25) Samorì, C.; Ali-Boucetta, H.; Sainz, R.; Guo, C.; Toma, F. M.; Fabbro, C.; da Ros, T.; Prato, M.; Kostarelos, K.; Bianco, A. Enhanced anticancer activity of multi-walled carbon nanotube-methotrexate conjugates using cleavable linkers. *Chem. Commun.* **2010**, *46* (9), 1494−1496.
(26) Draenert, F. G.; Draenert, K. Methotrexate-loaded polymethylmethacrylate bone cement for local bone metastasis therapy: pilot animal study in the rabbit patellar groove. *Chemotherapy* **2008**, *54* (5), 412−416.
(27) Maccauro, G.; Cittadini, A.; Casarci, M.; Muratori, F.; De Angelis, D.; Piconi, C.; Rosa, M. A.; Spadoni, A.; Braden, M.; Sgambato, A. Methotrexate-added acrylic cement: biological and physical properties. *J. Mater. Sci.: mater. Med.* **2007**, *18* (5), 839−844.
(28) Cai, B.; Liao, A.; Lee, K. K.; Ban, J. S.; Yang, H. S.; Im, Y. J.; Chun, C. Design, synthesis of methotrexate-diosgenin conjugates and biological evaluation of their effect on methotrexate transport-resistant cells. *Steroids* **2016**, *116*, 45−51.
(29) Yamashita, S.; Katsumi, H.; Sakane, T.; Yamamoto, A. Bone-targeting dendrimer for the delivery of methotrexate and treatment of bone metastasis. *J. Drug Target.* **2018**, *26* (9), 818−828.
(30) Cole, L. E.; Vargo-Gogola, T.; Roeder, R. K. Targeted delivery to bone and mineral deposits using bisphosphonate ligands. *Adv. Drug Delivery Rev.* **2016**, *99* (Pt A), 12−27.
(31) Xing, L.; Ebetino, F. H.; Boeckman, R. K., Jr.; Srinivasan, V.; Tao, J.; Sawyer, T. K.; Li, J.; Yao, Z.; Boyce, B. F. Targeting anti-cancer agents to bone using bisphosphonates. *Bone* **2020**, *138*, 115492.
(32) Sowers, R.; Wenzel, B. D.; Richardson, C.; Meyers, P. A.; Healey, J. H.; Levy, A. S.; Gorlick, R. Impairment of methotrexate transport is common in osteosarcoma tumor samples. *Sarcoma* **2011**, *2011*, 834170.
(33) Fujisaki, J.; Tokunaga, Y.; Takahashi, T.; Kimura, S.; Shimojo, F.; Hata, T. Osteotropic drug delivery system (ODDS) based on bisphosphonic prodrug. V. Biological disposition and targeting characteristics of osteotropic estradiol. *Biol. Pharm. Bull.* **1997**, *20* (11), 1183−1187.
(34) Fujisaki, J.; Tokunaga, Y.; Takahashi, T.; Shimojo, F.; Kimura, S.; Hata, T. Osteotropic drug delivery system (ODDS) based on bisphosphonic prodrug. I.v. effects of osteotropic estradiol on bone mineral density and uterine weight in ovariectomized rats. *J. Drug Target.* **1998**, *5* (2), 129−138.
(35) Fleisch, H. Bisphosphonates: a new class of drugs in diseases of bone and calcium metabolism. *Recent Results Cancer Res.* **1989**, *116*, 1−28.
(36) Erez, R.; Ebner, S.; Attali, B.; Shabat, D. Chemotherapeutic bone-targeted bisphosphonate prodrugs with hydrolytic mode of activation. *Bioorg. Med. Chem. Lett.* **2008**, *18* (2), 816−820.
(37) Hochdörffer, K.; Abu Ajaj, K.; Schäfer-Obodozie, C.; Kratz, F. Development of novel bisphosphonate prodrugs of doxorubicin for targeting bone metastases that are cleaved pH dependently or by cathepsin B: synthesis, cleavage properties, and binding properties to hydroxyapatite as well as bone matrix. *J. Med. Chem.* **2012**, *55* (17), 7502−7515.
(38) El-Mabhouh, A. A.; Angelov, C. A.; Cavell, R.; Mercer, J. R. A 99mTc-labeled gemcitabine bisphosphonate drug conjugate as a probe to assess the potential for targeted chemotherapy of metastatic bone cancer. *Nucl. Med. Biol.* **2006**, *33* (6), 715−722.
(39) El-Mabhouh, A. A.; Mercer, J. R. 188Re-labelled gemcitabine/bisphosphonate (Gem/BP): a multi-functional, bone-specific agent as a potential treatment for bone metastases. *Eur. J. Nucl. Med. Mol. Imaging* **2008**, *35* (7), 1240−1248.
(40) El-Mabhouh, A. A.; Nation, P. N.; Abele, J. T.; Riauka, T.; Postema, E.; McEwan, A. J.; Mercer, J. R. A conjugate of gemcitabine with bisphosphonate (Gem/BP) shows potential as a targeted bone-

https://doi.org/10.1021/acsomega.4c06029
ACS Omega 2024, 9, 42433−42447

specific therapeutic agent in an animal model of human breast cancer bone metastases. *Oncol. Res.* **2011**, *19* (6), 287−295.
(41) Andreeva, O. I.; Efimtseva, E. V.; Padiukova, N. S.; Kochetkov, S. N.; Mikhailov, S. N.; Dixon, G. B.; Karpeiskii, M. I. Vzaimodeistvie obratnoi transkriptazy VICh-1 i RNK-polimerazy bakteriofaga T7 s fosfonatnymi analogami NTP i neorganicheskogo pirofosfata [Interaction of HIV-1 reverse transcriptase and bacteriophage T7 RNA polymerase with NTP phosphonate analogs and inorganic pyrophosphate]. *Mol. Biol. (Mosk.)* **2001**, *35* (5), 844−856.
(42) Karpeisky, A.; Zinnen, S. Bone Targeted Therapeutics and Methods of Making and Using the Same. US 2009227544 A1, 2009.
(43) Ora, M.; Lönnberg, T.; Florea-Wang, D.; Zinnen, S.; Karpeisky, A.; Lönnberg, H. Bisphosphonate derivatives of nucleoside antimetabolites: hydrolytic stability and hydroxyapatite adsorption of 5′-beta,γ-methylene and 5′-beta,γ-(1-hydroxyethylidene) triphosphates of 5-fluorouridine and ara-cytidine. *J. Org. Chem.* **2008**, *73* (11), 4123−4130.
(44) Tanaka, K. S. E.; Dietrich, E.; Ciblat, S.; Métayer, C.; Arhin, F. F.; Sarmiento, I.; Moeck, G.; Parr, T. R., Jr.; Far, A. R. Synthesis and in vitro evaluation of bisphosphonated glycopeptide prodrugs for the treatment of osteomyelitis. *Bioorg. Med. Chem. Lett.* 2010, *20*, 4, 1355−1359
(45) Guervenou, J.; Sturtz, G. Synthese de conjugues gem-bisphosphoniques de derives de la cortisone. *Phosphorus, Sulfur Silicon Relat. Elem.* **1994**, *88* (1−4), 1−13.
(46) Hirabayashi, H.; Takahashi, T.; Fujisaki, J.; Masunaga, T.; Sato, S.; Hiroi, J.; Tokunaga, Y.; Kimura, S.; Hata, T. Bone-specific delivery and sustained release of diclofenac, a non-steroidal anti-inflammatory drug, via bisphosphonic prodrug based on the Osteotropic Drug Delivery System (ODDS). *J. Controlled Release* **2001**, *70* (1−2), 183−191.
(47) Hirabayashi, H.; Sawamoto, T.; Fujisaki, J.; Tokunaga, Y.; Kimura, S.; Hata, T. Relationship between physicochemical and osteotropic properties of bisphosphonic derivatives: rational design for osteotropic drug delivery system (ODDS). *Pharm. Res.* **2001**, *18* (5), 646−651.
(48) Gil, L.; Han, Y.; Opas, E. E.; Rodan, G. A.; Ruel, R.; Seedor, J. G.; Tyler, P. C.; Young, R. N. Prostaglandin E2-bisphosphonate conjugates: potential agents for treatment of osteoporosis. *Bioorg. Med. Chem.* **1999**, *7* (5), 901−919.
(49) Boeckman, R.; Boyce, B.; Xiao, L.; Yao, Z.; Ebetino, F. H. Phosphonate-Chloroquine Conjugates and Methods Using Same. WO 2017079260 A1, 2017.
(50) Mazess, R.; Bishop, C. Targeted therapeutic delivery of vitamin D compounds. US2003129194A1, 2003.
(51) Bauss, F.; Esswein, A.; Reiff, K.; Sponer, G.; Müller-Beckmann, B. Effect of 17beta-estradiol-bisphosphonate conjugates, potential bone-seeking estrogen pro-drugs, on 17beta-estradiol serum kinetics and bone mass in rats. *Calcif. Tissue Int.* **1996**, *59* (3), 168−173.
(52) Page, P. C. B.; Moore, J. P. G.; Mansfield, I.; McKenzie, M. J.; Bowler, W. B.; Gallagher, J. A. Synthesis of bone-targeted oestrogenic compounds for the inhibition of bone resorption. *Tetrahedron* **2001**, *57* (9), 1837−1847.
(53) Page, P. C.; McKenzie, M. J.; Gallagher, J. A. Novel synthesis of bis(phosphonic acid)-steroid conjugates. *J. Org. Chem.* **2001**, *66* (11), 3704−3708.
(54) Morioka, M.; Kamizono, A.; Takikawa, H.; Mori, A.; Ueno, H.; Kadowaki, S.; Nakao, Y.; Kato, K.; Umezawa, K. Design, synthesis, and biological evaluation of novel estradiol-bisphosphonate conjugates as bone-specific estrogens. *Bioorg. Med. Chem.* **2010**, *18* (3), 1143−1148.
(55) Tanaka, K. S. E.; Houghton, T. J.; Kang, T.; Dietrich, E.; Delorme, D.; Ferreira, S. S.; Caron, L.; Viens, F.; Arhin, F. F.; Sarmiento, I.; et al. Bisphosphonated fluoroquinolone esters as osteotropic prodrugs for the prevention of osteomyelitis. *Bioorg. Med. Chem.* **2008**, *16* (20), 9217−9229.
(56) Houghton, T. J.; Tanaka, K. S. E.; Kang, T.; Dietrich, E.; Lafontaine, Y.; Delorme, D.; Ferreira, S. S.; Viens, F.; Arhin, F. F.; Sarmiento, I.; et al. Linking bisphosphonates to the free amino groups in fluoroquinolones: preparation of osteotropic prodrugs for the prevention of osteomyelitis. *J. Med. Chem.* **2008**, *51* (21), 6955−6969.
(57) Ebetino, F. H.; Sun, S.; Lundy, M. W.; McKenna, C. E.; Richard, E.; Sedghizadeh, P.; Sadrerafi, K. Bisphosphonate quinolone conjugates and uses thereof. WO 2017210611 A1, 2017.
(58) Sedghizadeh, P. P.; Sun, S.; Junka, A. F.; Richard, E.; Sadrerafi, K.; Mahabady, S.; Bakhshalian, N.; Tjokro, N.; Bartoszewicz, M.; Oleksy, M.; et al. Design, Synthesis, and Antimicrobial Evaluation of a Novel Bone-Targeting Bisphosphonate-Ciprofloxacin Conjugate for the Treatment of Osteomyelitis Biofilms. *J. Med. Chem.* **2017**, *60* (6), 2326−2343.
(59) Reddy, R.; Dietrich, E.; Lafontaine, Y.; Houghton, T. J.; Belanger, O.; Dubois, A.; Arhin, F. F.; Sarmiento, I.; Fadhil, I.; Laquerre, K.; et al. Bisphosphonated benzoxazinorifamycin prodrugs for the prevention and treatment of osteomyelitis. *ChemMedChem* **2008**, *3* (12), 1863−1868.
(60) Egorov, M.; Fortun, Y.; Heymann, D.; Lebreton, J.; Mathe, M.; Padrines, M.; Redini, F.Hydroxy-bisphosphonic acid derivatives as vector for targeting bone tissue. WO 2009083614A1, 2009.
(61) Egorov, M.; Goujon, J.-Y.; Le Bot, R. Bifunctional hydroxybisphosphonic acid derivatives. WO2012130911A1, 2012.
(62) Zinnen, S. P.; Karpeisky, A.; Von Hoff, D. D.; Plekhova, L.; Alexandrov, A. First-in-Human Phase I Study of MBC-11, a Novel Bone-Targeted Cytarabine-Etidronate Conjugate in Patients with Cancer-Induced Bone Disease. *Oncologist* **2019**, *24* (3), 303−e102.
(63) Ye, W. L.; Zhao, Y. P.; Na, R.; Li, F.; Mei, Q. B.; Zhao, M. G.; Zhou, S. Y. Actively targeted delivery of doxorubicin to bone metastases by a pH-sensitive conjugation. *J. Pharm. Sci.* **2015**, *104* (7), 2293−2303.
(64) Egorov, M.; Goujon, J.-Y.; Le Bot, R.; David, E. Hydrosoluble hydroxybisphosphonic derivatives of doxorubicin. WO2016079327A1, 2016.
(65) David, E.; Cagnol, S.; Goujon, J. Y.; Egorov, M.; Taurelle, J.; Benesteau, C.; Morandeau, L.; Moal, C.; Sicard, M.; Pairel, S.; Heymann, D.; Redini, F.; Gouin, F.; Le Bot, R. 12b80−Hydroxybisphosphonate Linked Doxorubicin: Bone Targeted Strategy for Treatment of Osteosarcoma. *Bioconjugate Chem.* **2019**, *30* (6), 1665−1676.
(66) Metcalf, C.; Rozamus, L.; Wang, Y.; Thomas, R.; Zou, D.; Berstein, D. Phosphorus-containing macrocycles. US 2006264405 A1, 2006.
(67) Egorov, M.; Cagnol, S.; Le Bot, R.; Goujon, J.-Y. Hydroxybisphosphonic derivatives of meloxicam for the treatment of inflammatory joint diseases. WO2022229576A1, 2022.
(68) Aoun, S.; Sierocki, P.; Lebreton, J.; Mathé-Allainmat, M. Linear and Convergent Syntheses of Bifunctional Hydroxy-Bisphosphonic Compounds as Potential Bone-Targeting Prodrugs. *Synthesis* **2019**, *51* (18), 3556−3566.
(69) Arns, S.; Gibe, R.; Moreau, A.; Monzur Morshed, M.; Young, R. N. Design and synthesis of novel bone-targeting dual-action pro-drugs for the treatment and reversal of osteoporosis. *Bioorg. Med. Chem.* **2012**, *20* (6), 2131−2140.
(70) Chen, G.; Arns, S.; Young, R. N. Determination of the rat *in vivo* pharmacokinetic profile of a bone-targeting dual-action pro-drug for treatment of osteoporosis. *Bioconjugate Chem.* **2015**, *26* (6), 1095−1103.
(71) Xie, H.; Chen, G.; Young, R. N. Design, Synthesis, and Pharmacokinetics of a Bone-Targeting Dual-Action Prodrug for the Treatment of Osteoporosis. *J. Med. Chem.* **2017**, *60* (16), 7012−7028.
(72) Ebetino, F. H.; Hogan, A. M.; Sun, S.; Tsoumpra, M. K.; Duan, X.; Triffitt, J. T.; Kwaasi, A. A.; Dunford, J. E.; Barnett, B. L.; Oppermann, U.; et al. The relationship between the chemistry and biological activity of the bisphosphonates. *Bone* **2011**, *49* (1), 20−33.
(73) Chou, A. J.; Geller, D. S.; Gorlick, R. Therapy for osteosarcoma: where do we go from here? *Paediatr. Drugs* **2008**, *10* (5), 315−327.
(74) Farrell, K. B.; Karpeisky, A.; Thamm, D. H.; Zinnen, S. Bisphosphonate conjugation for bone specific drug targeting. *Bone Rep.* **2018**, *9*, 47−60.

https://doi.org/10.1021/acsomega.4c06029
ACS Omega 2024, 9, 42433−42447

(75) Sturtz, G.; Appéré, G.; Breistol, K.; Fodstad, O.; Schwartsmann, G.; Hendriks, H. R. A study of the delivery-targeting concept applied to antineoplastic drugs active on human osteosarcoma. I. Synthesis and biological activity in nude mice carrying human osteosarcoma xenografts of gem-bisphosphonic methotrexate analogues. *Eur. J. Med. Chem.* **1992**, *27* (8), 825−833.
(76) Sturtz, G.; Couthon, H.; Fabulet, O.; Mian, M.; Rosini, S. Synthesis of gem-Bisphosphonic Methotrexate Conjugates and Their Biological Response Towards Walker's Osteosarcoma. *Eur. J. Med. Chem.* **1993**, *28* (11), 899−903.
(77) Kratz, F. Bisphosphonate-prodrugs. WO 2011023367 A2, 2011.
(78) Boyé, P.; David, E.; Serres, F.; Pascal, Q.; Floch, F.; Geeraert, K.; Coste, V.; Marescaux, L.; Cagnol, S.; Goujon, J. Y.; Egorov, M.; Le Bot, R.; Tierny, D. Phase I dose escalation study of 12b80 (hydroxybisphosphonate linked doxorubicin) in naturally occurring osteosarcoma. *Oncotarget* **2020**, *11* (46), 4281−4292.
(79) Wingen, F.; Pool, B. L.; Klein, P.; Klenner, T.; Schmähl, D. Anticancer activity of bisphosphonic acids in methylnitrosourea-induced mammary carcinoma of the rat-benefit of combining bisphosphonates with cytostatic agents. *Invest. New Drugs* **1988**, *6* (3), 155−167.
(80) Wingen, F.; Eichmann, T.; Manegold, C.; Krempien, B. Effects of new bisphosphonic acids on tumor-induced bone destruction in the rat. *J. Cancer Res. Clin Oncol.* **1986**, *111* (1), 35−41.
(81) Drago, C.; Arosio, D.; Casagrande, C.; Manzoni, L. Bisphosphonate-functionalized cyclic Arg-Gly-Asp peptidomimetics. *ARKIVOC* **2013**, *2013* (2), 185−200.
(82) Liu, X. M.; Lee, H. T.; Reinhardt, R. A.; Marky, L. A.; Wang, D. Novel biomineral-binding cyclodextrins for controlled drug delivery in the oral cavity. *J. Controlled Release* **2007**, *122* (1), 54−62.
(83) Egorov, M.; Aoun, S.; Padrines, M.; Redini, F.; Heymann, D.; Lebreton, J.; Mathe-Allainmat, M. A One-Pot Synthesis of 1-Hydroxy-1,1-bis(phosphonic acid)s Starting from the Corresponding Carboxylic Acids. *Eur. J. Org. Chem.* **2011**, 7148−7154.
(84) Egorov, M.; Fortun, Y.; Heymann, D.; Lebreton, J.; Mathe, M.; Padrines, M.; Redini, F. Method for synthesizing hydroxy-bisphosphonic acid derivatives. WO2009083613A1, 2009.
(85) Hosain, F.; Spencer, R. P.; Couthon, H. M.; Sturtz, G. L. Targeted delivery of antineoplastic agent to bone: biodistribution studies of technetium-99m-labeled gem-bisphosphonate conjugate of methotrexate. *J. Nucl. Med.* **1996**, *37* (1), 105−107.
(86) van Beek, E. R.; Löwik, C. W.; Ebetino, F. H.; Papapoulos, S. E. Binding and antiresorptive properties of heterocycle-containing bisphosphonate analogs: structure-activity relationships. *Bone* **1998**, *23* (5), 437−442.
(87) Widler, L.; Jaeggi, K. A.; Glatt, M.; Müller, K.; Bachmann, R.; Bisping, M.; Born, A.-R.; Cortesi, R.; Guiglia, G.; Jeker, H.; et al. Highly potent geminal bisphosphonates. From pamidronate disodium (Aredia) to zoledronic acid (Zometa). *J. Med. Chem.* **2002**, *45* (17), 3721−3738.
(88) Francis, C. L.; Yang, Q.; Hart, N. K.; Widmer, F.; Manthey, M. K.; He-Williams, H. M. Total Synthesis of Methotrexate-γ-TRIS-Fatty Acid Conjugates. *Aust. J. Chem.* **2002**, *55* (10), 635−645.
(89) Carrasco, M. P.; Enyedy, E. A.; Krupenko, N. I.; Krupenko, S. A.; Nuti, E.; Tuccinardi, T.; Santamaria, S.; Rossello, A.; Martinelli, A.; Santos, M. A. Novel folate-hydroxamate based antimetabolites: synthesis and biological evaluation. *Med. Chem.* **2011**, *7* (4), 265−274.
(90) Piper, J. R.; Montgomery, J. A.; Sirotnak, F. M.; Chello, P. L. Syntheses of α- and γ-substituted amides, peptides, and esters of methotrexate and their evaluation as inhibitors of folate metabolism. *J. Med. Chem.* **1982**, *25* (2), 182−187.
(91) Rosowsky, A.; Freisheim, J. H.; Bader, H.; Forsch, R. A.; Susten, S. S.; Cucchi, C. A.; Frie, E., III Methotrexate analogues. 25. Chemical and biological studies on the γ-tert-butyl esters of methotrexate and aminopterin. *J. Med. Chem.* **1985**, *28* (5), 660−667.
(92) Fabulet, O.; Sturtz, G. Synthesis of gem-bisphosphonic doxorubicin conjugates. *Phosphorus, Sulfur Silicon Relat. Elem.* **1995**, *101* (1−4), 225−234.
(93) Kuefner, U.; Lohrmann, U.; Montejano, Y. D.; Vitols, K. S.; Huennekens, F. M. Carboxypeptidase-mediated release of methotrexate from methotrexate α-peptides. *Biochemistry* **1989**, *28* (5), 2288−2297.
(94) Hein, C. D.; Liu, X. M.; Chen, F.; Cullen, D. M.; Wang, D. The synthesis of a multiblock osteotropic polyrotaxane by copper(I)-catalyzed huisgen 1,3-dipolar cycloaddition. *Macromol. Biosci.* **2010**, *10* (12), 1544−1556.
(95) Fitch, S. J.; Moedritzer, K. N.m.r. Study of the P-C(OH)-P to P-C-O-P Rearrangement: Tetraethyl 1-Hydroxyalkylidenediphosphonates. *J. Am. Chem. Soc.* **1962**, *84* (10), 1876−1879.
(96) Griffiths, D. V.; Hughes, J. M.; Brown, J. W.; Caesar, J. C.; Swetnam, S. P.; Cumming, S. A.; Kelly, J. D. The synthesis of 1-amino-2-hydroxy- and 2-amino-1-hydroxy-substituted ethylene-1,1-bisphosphonic acids and their N-methylated derivatives. *Tetrahedron* **1997**, *53* (52), 17815−17822.
(97) Vachal, P.; Hale, J. J.; Lu, Z.; Streckfuss, E. C.; Mills, S. G.; MacCoss, M.; Yin, D. H.; Algayer, K.; Manser, K.; Kesisoglou, F.; Ghosh, S.; Alani, L. L. Synthesis and study of alendronate derivatives as potential prodrugs of alendronate sodium for the treatment of low bone density and osteoporosis. *J. Med. Chem.* **2006**, *49* (11), 3060−3063.
(98) Turhanen, P. A. Synthesis of triple-bond-containing 1-hydroxy-1,1-bisphosphonic acid derivatives to be used as precursors in "click" chemistry: two examples. *J. Org. Chem.* **2014**, *79* (13), 6330−6335.
(99) McKenna, C. E.; Higa, M. T.; Cheung, N. H.; McKenna, M. C. The facile dealkylation of phosphonic acid dialkyl esters by bromotrimethylsilane. *Tetrahedron Lett.* **1977**, *18* (2), 155−158.
(100) McKenna, C. E.; Schmidhuser, J. Functional selectivity in phosphonate ester dealkylation with bromotrimethylsilane. *J. Chem. Soc., Chem. Commun.* **1979**, 739−739.
(101) Rapposelli, S.; Gambari, L.; Digiacomo, M.; Citi, V.; Lisignoli, G.; Manferdini, C.; Calderone, V.; Grassi, F. A Novel H2S-releasing Amino-Bisphosphonate which combines bone anti-catabolic and anabolic functions. *Sci. Rep.* **2017**, *7* (1), 11940.
(102) Lecouvey, M.; Mallard, I.; Bailly, T.; Burgada, R.; Leroux, Y. A mild and efficient one-pot synthesis of 1-hydroxymethylene-1,1-bisphosphonic acids. Preparation of new tripod ligands. *Tetrahedron Lett.* **2001**, *42*, 8475−8478.
(103) Guénin, E.; Monteil, M.; Bouchemal, N.; Prangé, T.; Lecouvey, M. Syntheses of Phosphonic Esters of Alendronate, Pamidronate and Neridronate. *Eur. J. Org. Chem.* **2007**, *20*, 3380−3391.
(104) Choi, S. K.; Verma, M.; Silpe, J.; Moody, R. E.; Tang, K.; Hanson, J. J.; Baker, J. R., Jr. A photochemical approach for controlled drug release in targeted drug delivery. *Bioorg. Med. Chem.* **2012**, *20* (3), 1281−1290.
(105) Kuefner, U.; Esswein, A.; Lohrmann, U.; Montejano, Y.; Vitols, K. S.; Huennekens, F. M. Occurrence and significance of diastereomers of methotrexate α-peptides. *Biochemistry* **1990**, *29* (46), 10540−10545.
(106) Totani, K.; Matsuo, I.; Ito, Y. Tight binding ligand approach to oligosaccharide-grafted protein. *Bioorg. Med. Chem. Lett.* **2004**, *14* (9), 2285−2289.
(107) Poe, M. Acidic dissociation constants of folic acid, dihydrofolic acid, and methotrexate. *J. Biol. Chem.* **1977**, *252* (11), 3724−3728.
(108) Nefkens, G. H. L.; Nivard, R. J. F. A new method for the synthesis of α-esters of N-acylglutamic acids. *Recl. Trav. Chim. Pays-Bas* **1964**, *83* (2), 199−207.
(109) Fitzhugh, A. L.; Akee, R. K.; Ruei, F. C.; Wu, J.; Klose, J. R.; Chabner, B. A. First completely chemical synthesis of [(6S)-N5-formyltetrahydropteroyl]poly γ-L-glutamic acid derivatives. *J. Chem. Soc., Perkin Trans. 1* **1994**, *1* (7), 897−902.
(110) Rosowsky, A.; Forsch, R. A.; Yu, C. S.; Lazarus, H.; Beardsley, G. P. Methotrexate analogues. 21. Divergent influence of alkyl chain length on the dihydrofolate reductase affinity and cytotoxicity of methotrexate monoesters. *J. Med. Chem.* **1984**, *27* (5), 605−609.

https://doi.org/10.1021/acsomega.4c06029
ACS Omega 2024, 9, 42433−42447